



Deposited via The University of Sheffield.

White Rose Research Online URL for this paper:

<https://eprints.whiterose.ac.uk/id/eprint/97659/>

Version: Accepted Version

Article:

Ghadbeigi, H., Pinna, C. and Celotto, S. (2012) Quantitative strain analysis of the large deformation at the scale of microstructure: comparison between Digital Image Correlation and Microgrid techniques. *Experimental Mechanics*, 52 (9). pp. 1483-1492. ISSN: 0014-4851

<https://doi.org/10.1007/s11340-012-9612-6>

Reuse

Items deposited in White Rose Research Online are protected by copyright, with all rights reserved unless indicated otherwise. They may be downloaded and/or printed for private study, or other acts as permitted by national copyright laws. The publisher or other rights holders may allow further reproduction and re-use of the full text version. This is indicated by the licence information on the White Rose Research Online record for the item.

Takedown

If you consider content in White Rose Research Online to be in breach of UK law, please notify us by emailing eprints@whiterose.ac.uk including the URL of the record and the reason for the withdrawal request.

Quantitative strain analysis of the large deformation at the scale of microstructure: comparison between Digital Image Correlation and Microgrid techniques

H. Ghadbeigi^{a*}, C. Pinna^a, S. Celotto^b

^a *The University of Sheffield, Department of Mechanical Engineering,
Mappin Street, Sheffield, S1 3JD, UK*

^b *Tata Steel RD&T, IJmuiden, The Netherlands*

* *Corresponding author: h.ghadbeigi@sheffield.ac.uk*

Tel: +44 (0) 114 222 7862

Fax: +44 (0) 114 222 7890

Abstract

A comparative study has been carried out to assess the accuracy of the Digital Image Correlation (DIC) technique for the quantification of large strains in the microstructure of a Interstitial Free (IF) steel used in automotive applications. A microgrid technique has been used in this study in order to validate independently the strain measurements obtained with DIC. Microgrids with a pitch of 5 microns were printed on the etched microstructure of the IF steel to measure the local in-plane strain distribution during a tensile test carried out in a Scanning Electron Microscope (SEM). The progressive deformation of the microstructure with microgrids has been recorded throughout the test as a sequence of micrographs and subsequently processed using DIC to quantify the distribution of local strain values. Strain maps obtained with the two techniques have been compared in order to assess the accuracy of the DIC measurements obtained using the natural patterns of the revealed microstructure in the SEM micrographs. Although results obtained with the two techniques are qualitatively similar, therefore demonstrating the reliability of DIC applied to microstructures, even after large deformations in excess of 0.7. However, an average error of about 16% was found in the strain values calculated using DIC.

Keywords: Mechanical testing, Digital image correlation, Microgrid, Interstitial free (IF) steel

1 Introduction

The development of reliable models of deformation and damage of microstructures of materials requires insight from experimental techniques that are capable of quantifying strain distributions at the local scale [1]. The micro-scale deformation of materials has been mostly studied through the observation of microstructural evolution using different techniques including in-situ mechanical testing combined with strain measurements at a microscopic scale [2-5] with the aim to relate local strain distributions within microstructural constituents to identified deformation mechanisms [6-8]. Allais *et al.* [9] developed a technique to measure strain distributions from the distortion of microgrids laid onto the surface of dual-phase materials, i.e. iron/silver and iron/copper alloys, using tensile specimens deformed in a SEM. The electron beam lithography technique was used to print microgrids of gold dots with a pitch of 5 μ m. Other methods including electro-polishing [10], photolithography [11], electro-resist method [12] and deposition [13] have also been used to print microgrids onto the surface of materials in order to measure strain distributions due to plastic deformation [10,14] as well as strain fields around a crack tip [15] with different resolutions. According to one study [9], the microgrid technique enables to accurately measure strain distributions in

the microstructure of a deformed material since microgrids directly follow the very local deformation of microstructures. Despite its accuracy, the application of the microgrid method is limited as a result of technical difficulties associated with the production of sub-micron grids [16]. The DIC technique has been used to overcome the problems associated with the production of grids and has been successfully applied to both macro and micro scales studies as a non-contact method to measure strain distributions in deformed specimens [17-21]. Sun and co-workers [22] developed a procedure with a displacement accuracy of about 1 μ m to measure the in-plane microscopic deformation of an aluminium alloy during tensile deformation. They analysed optical micrographs of the surface of the deforming sample using the DIC technique to obtain strain maps of the analysed region with strain values up to 5 micro-strains. In recent years, the DIC technique has been widely used to quantify the microstructural deformation [2,8]. However, the application of random speckle patterns is practically restricted at this scale, therefore SEM micrographs have been used together with DIC [8,23,24] to measure strain distributions within the microstructure of both dual [2] and single [5,24] phase materials, where the microstructure itself was used to correlate the images.

Although several developments have been made over the years to improve the algorithms for image processing, e.g. [21,25,26], few studies have been carried out to validate the strain field measured at the microstructural scale, especially under large deformation, through a comparison with results obtained from a separate experimental technique [21].

Jin et al [27] investigated both the grid method and the DIC technique to measure the discontinuous displacement field around the tip of a propagating crack at relatively low magnifications. The applied deformation was in the range of linear elastic deformation and no quantitative comparison was made between the results obtained from DIC and those obtained with their grid technique.

Even though some work has been done to assess the accuracy of the measured displacement field with the DIC technique [18,28-30], no quantitative analysis has been done in the case of very large local deformation to the authors' knowledge.

Kang and co-workers [5] performed a comparison study to verify the accuracy of strain values measured using DIC during an in-situ tensile test where the microstructure of the specimen was used to correlate the images. They compared average strain values determined by DIC with an initial gauge length of about 100 μ m with those calculated by measuring the change in indent spacing that were initially 0.25 mm apart, made on the surface of the specimen. Although they showed that for the 25 % applied strain the difference in measured global strain value was about ± 10 % between the two methods, the local strain values were not considered in the comparison.

The present study has been carried out to quantify strain values at the scale of the microstructure of a single phase automotive steel during in-situ tensile testing using both DIC and microgrid techniques in order to assess the accuracy of the strain measurements obtained with DIC.

2 Experimental procedure

In order to investigate the reliability of local strain maps determined with the DIC technique, an in-situ tensile testing procedure developed by the authors [31] has been used. The micro-tensile specimen, Fig. 1-a, is loaded inside the chamber of a SEM while micrographs of the deformed microstructure are taken at regular intervals. The images are then processed using

the commercial DIC software LAvision using the natural pattern of the microstructure in order to compute strain values. The methodology enables the determination of local strain values at the surface of tensile specimens up to final fracture. A commercial IF steel produced as sheets with a thickness of about 1 mm was used to manufacture the specimens, Fig. 1-a. The material is a single-phase ferritic steel and is used to produce car body panels. The great ductility of the IF steel results in large elongation to fracture and therefore, very large strain values are experienced during the tensile test. The surface of the specimen has been mechanically polished and chemically etched with the Marshall's etchant [32] for about 5 seconds prior to the tests in order to reveal the microstructure of the material. Fig. 1 shows the specimen and a scanning electron micrograph of the revealed microstructure. The micrograph of the etched specimen shows the optimal conditions found in terms of contrast generated at the grain boundaries in order to process the SEM images using DIC.

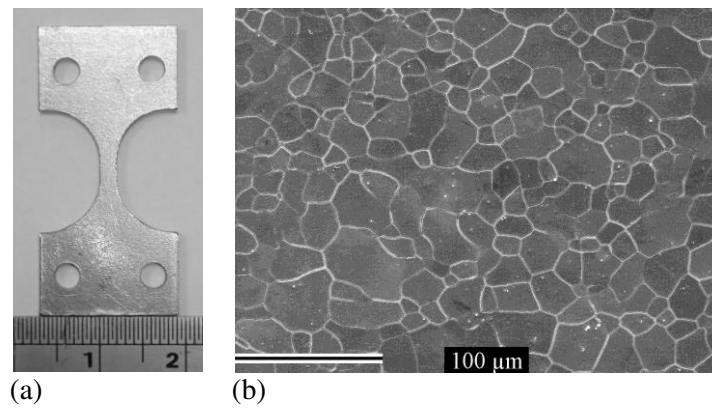


Fig. 1 (a) In-situ tensile test specimen and (b) the microstructure of IF steel revealed by using Marshall's etchant

After etching, Electron Beam Lithography technique [6,9] has been used to lay square microgrids of gold with a pitch of 5 microns on the surface of the specimen. The distortion of the grids during the test is used to determine the in-plane components of the local deformation gradient tensor under the framework of large strain deformation. The local true plastic strain maps are then calculated according to the procedure given in [6].

The tensile test has been carried out at a displacement rate of $2.66 \mu\text{m s}^{-1}$ with steps of $30\mu\text{m}$. After each step, the test was interrupted and the specimen was moved to its initial position to have the same observation region inside the SEM chamber and a micrograph of the deformed microstructure was taken. The commercial package LaVision [33] has been used to perform the DIC analysis on the micrographs of the deformed microstructure. The selected region for the DIC analysis covers an area of about $219\mu\text{m} \times 163\mu\text{m}$ at the very centre of the gauge section of the tensile specimen. A multi-pass algorithm [33] was used to perform the image correlation. In the first pass, a square interrogation window with a size of $63 \mu\text{m} \times 63 \mu\text{m}$ was selected, while a $7.86 \mu\text{m} \times 7.86 \mu\text{m}$ window, corresponding to 32×32 pixels in the micrograph, was used in the second pass. The overlap between two adjacent windows was 25% and 50% for the first and second passes respectively. As a result a spatial resolution of about $6 \mu\text{m}$ was achieved, which also corresponds to the gauge length used in the DIC technique for strain calculations. This combination of optimized parameters was selected to obtain a gauge length as close as possible to that of the printed microgrids in order to achieve a reliable comparison between the measurements obtained from the two independent techniques [33]. The strain values were computed from the in-plane displacement field

obtained from the DIC analysis. The tensile test was stopped in the middle of the post uniform plastic deformation due to the large amount of out of plane deformation experienced in the selected region of the microstructure. This out-of-plane deformation caused a large variation of contrast and brightness in the micrographs that was indeed detrimental to the correlation results. The last micrograph taken was used to plot the total in-plane plastic strain maps on the deformed configuration of the microstructure. The strain maps determined by using the DIC and microgrid techniques have then been compared to assess the accuracy of the strain values computed using DIC on micrographs.

3 Results

The load-elongation curve recorded during the test from the tensile stage is shown in Fig. 2. The small drops in the tensile load correspond to the stress relaxation experienced by the specimen, assuming that the apparatus is rigid compared with the specimen, due to regular interruptions of the test in order to record the images. Figure 3a shows the undeformed grids before the test while Figure 3b shows the extent of deformation after an applied strain value of about 0.73 over the region of the microstructure selected for strain analysis.

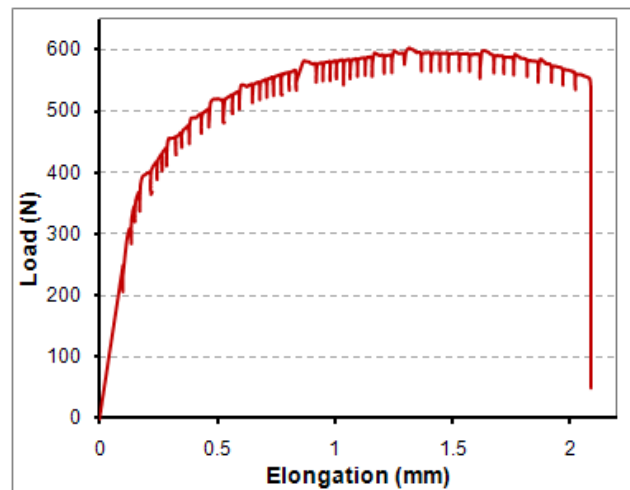


Fig. 2 Load-elongation curve obtained from the in-situ tensile test

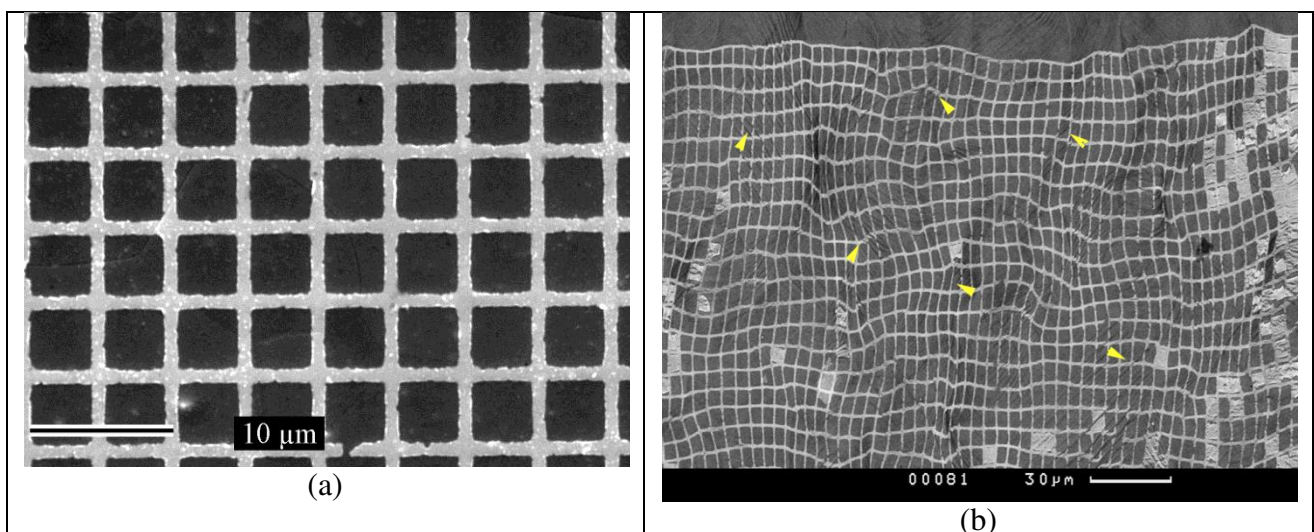


Fig. 3 Micrographs of (a) undeformed grids and (b) deformed microstructure that shows the distortion of the microgrids together with severe local shearing in the microstructure highlighted by the arrows. Discrete slip lines parallel to each other are visible as sharp dark lines aligned 45° to the horizontal edge.

3.1 Digital Image Correlation

Fig. 4-a shows the severe deformation localisation and local shearing of the microstructure after the applied strain, wherein shear bands and even sharp linear slip lines are well visible in the distorted microgrids. Fig.4-b shows the result of image correlation for displacement vectors superimposed onto the microstructure after an applied true strain of 0.73. This was the maximum value for which the correlation worked. The colour scale in Fig. 4-b shows the displacement distribution of the pixels located at the centre of the interrogation windows. The map indicates that despite a severe deformation localisation within the microstructure (Fig. 4-a), a good correlation has been obtained during the image processing using the optimum parameters found after several trial and errors.

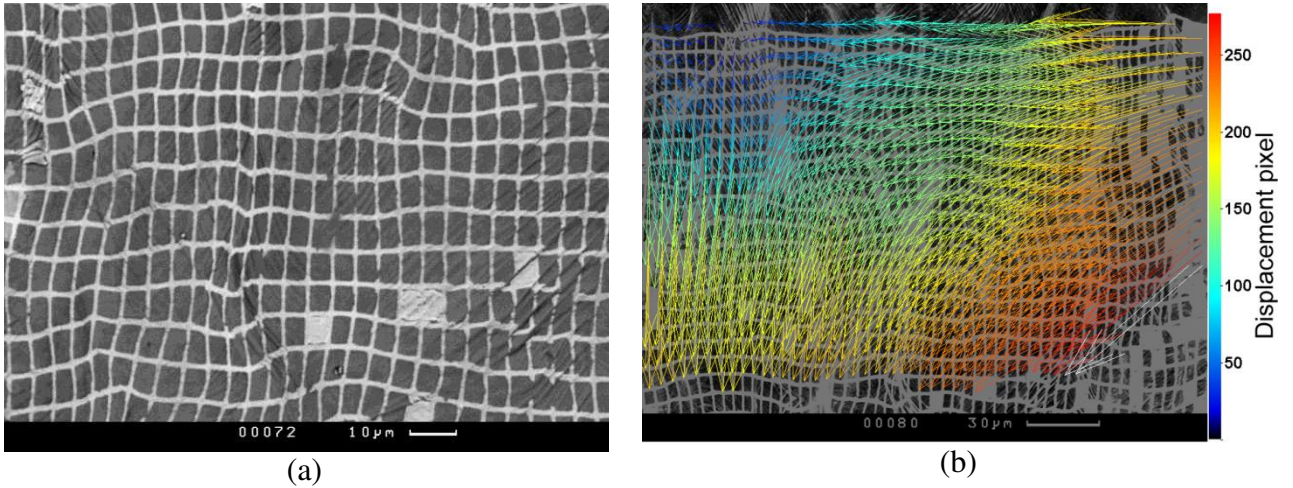


Fig.4 (a) micrograph of the deformed microstructure showing a severe deformation localisation and local shear bands in the grains and (b) the displacement vector map obtained from the DIC analysis of the microstructure pattern

The strain values are calculated based on the definition of the normal engineering strains, equation 1, in the LAvision program that includes both the elastic and plastic strains. V in equation (1) is the total displacement vector for the pixel at the centre of each interrogation window in the first image, and r is the vector defining the undeformed grid size that is also the size of the gauge length for strain measurements. It is assumed that the elastic strains are negligible for large deformation and as a result, true strain values are calculated according to equation (2) where E is the engineering strain obtained from the total displacement vector calculated for the final image with reference to the undeformed configuration and ε is the true strain value. The computed strain maps for true (ε_{yy}) strains along the loading direction superimposed onto the deformed microstructure are shown in Fig.5.

$$E_{ij} = \frac{dV_i}{dr_j} \quad \text{with } i, j = x, y \quad (1)$$

$$\varepsilon = \ln(1 + E) \quad (2)$$

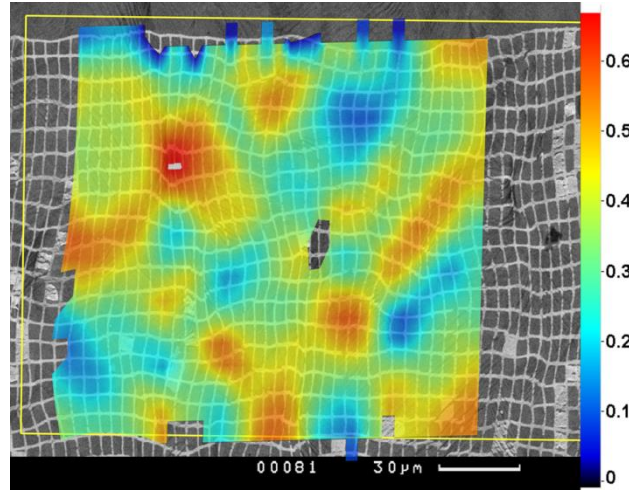


Fig.5 True in-plane strain maps in the loading direction obtained from the DIC results superimposed onto the deformed microstructure

The maps show that deformation within the microstructure of the tested material is heterogeneous with deformation bands observed at about 45° with respect to the loading direction. The obtained strain distributions show a reasonable agreement with the distortion pattern of the microgrids. Although Fig.4 showed that a good correlation was achieved, there are some parts of the strain map where the correlation has been lost due to severe deformation and changes in the gray contrast of the micrographs that occurred at the end of the test. Local strain values as large as 0.7 and 0.98 for the true and engineering strains, respectively, are measured whereas neighbouring grains experience local strain values smaller than 0.1. Such a large variation in strain values might be due to the effect of grain orientation in the microstructure of the IF steel.

3.2 The microgrid technique

Grids laid on the microstructure deformed during the in-situ tensile test and analysed using DIC have been used to directly measure strain values for an independent comparison.

Local in-plane true strain values have been computed using the deformed configuration of the microgrids according to the large deformation theory reported in [9]. The undeformed configuration of the grids is known before the test and the deformed configuration is determined by pinpointing the position of the grids intersections. The in-plane deformation gradient tensor, equation (3), can be decomposed into a rigid rotation tensor R and a distortion tensor U , equation (4).

$$F = \begin{pmatrix} x_1^I & x_1^{II} \\ x_2^I & x_2^{II} \end{pmatrix} \begin{pmatrix} X_1^I & X_1^{II} \\ X_2^I & X_2^{II} \end{pmatrix}^{-1} \quad (3)$$

$$F = R \cdot U \quad (4)$$

The vector coordinates in the deformed and undeformed configurations are denoted by x_i and X_i for $i=1,2$, respectively. U can be diagonalised in an orthogonal base using the following equation:

$$U = Q^t D Q \quad (5)$$

The logarithmic strain tensor is then computed from the diagonalised distortion tensor according to equation (6), where D represents the diagonal tensor and Q is a tensor giving the orientation of the principal directions of the distortion.

$$E^{Log} = Q^t \ln(D) Q \quad (6)$$

Fig. 6 shows the distribution of measured strain values along the loading direction for the same region as that shown in Fig.5. A similar colour scale has been used to simplify the comparison.

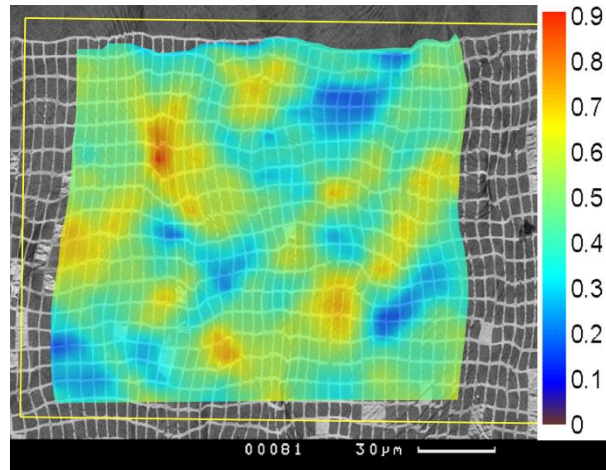


Fig.6 True plastic strain map obtained from the analysis of the deformed microgrids

The comparison of Fig.5 and Fig.6 shows that the strain map produced for the deformed microstructure by using DIC is in good qualitative agreement with the result obtained from the microgrid technique in terms of strain distribution patterns. However, the strain values are under-determined from the DIC technique. The difference in strain values results from the errors associated with the micrographs quality, electron beam effect, correlation algorithm as well as errors inherent to strain calculations using the microgrid technique, which is explained in the next section.

4 Discussion

The experimental procedure developed in this work has allowed strain maps to be produced after a large amount of deformation at the scale of microstructure. The microgrid technique provides an opportunity to assess the reliability of the strain measurements obtained using DIC at such fine scale.

A qualitative comparison of the strain maps obtained from the two techniques, Fig.5 and Fig.6, shows that the strain distribution pattern measured by the DIC technique matches the one that obtained using the microgrid technique. The difference in the measured strain values is related to the errors associated with the DIC and the microgrid techniques. These are: a) the uncertainty in pinpointing the deformed grids intersections to measure the strain distribution, E_G , b) errors due to beam shift in electron microscopy [28,29], E_B and c) the errors associated with the correlation algorithms in DIC[34].

An undeformed set of microgrids, Fig. 7-a, was used to quantify E_G as the maximum error value generated when clicking on grid intersections following the procedure described in [6]. The resulting strain map is shown in Fig. 7-b and shows that the error in the measured strain

values is distributed over the analysed region. A maximum absolute error value of 0.022 has been recorded and is therefore negligible compared to the large strain values of the order of 1 measured during the tensile test.

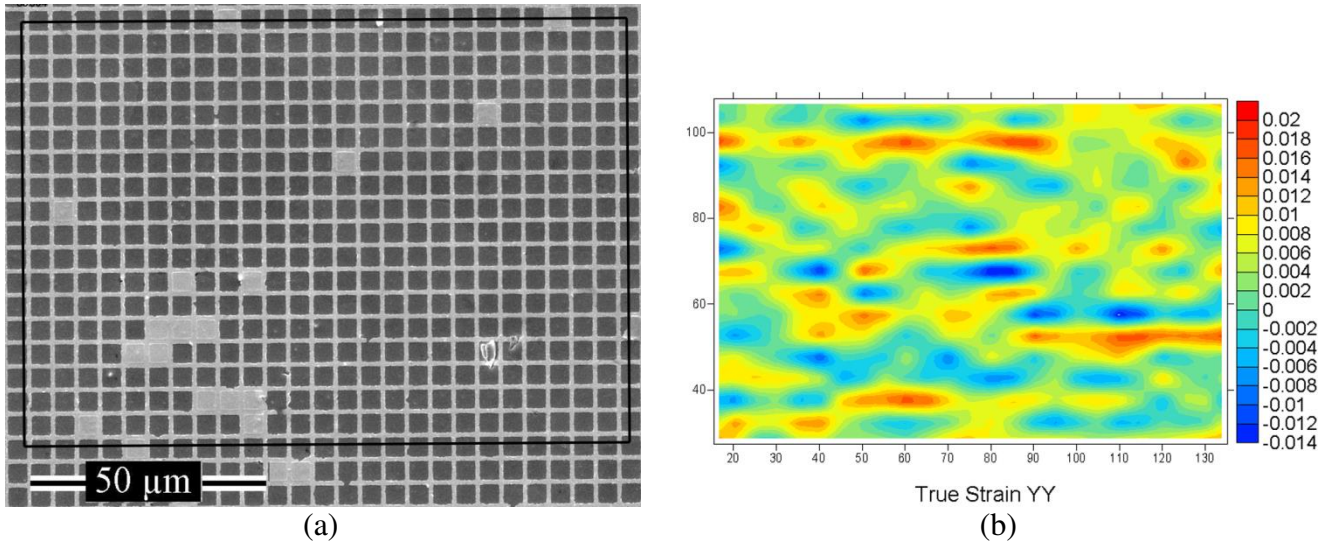


Fig. 7 (a) Undeformed microgrids and (b) the corresponding strain map used to measure E_G

The beam shift error occurs due to a time-dependent drift of the electron beam during scanning electron microscopy, which creates a generic and random error that is more prominent at higher magnifications [28]. Two micrographs of the undeformed microstructure taken with a time interval equal to the imaging time of the test, approximately 3 minutes, have been analysed with DIC to quantify the maximum error in the measured strain values due to the beam shift, E_B . Fig. 8 shows the resulting strain map with a maximum absolute strain value of 0.004, which is negligible compared to the strain values recorded during the test. This is likely to be due to the magnification selected to record the images, which is relatively low (about 500X) as the lower the magnification, the smaller the beam shift and consequently the smaller the error in strain measurement [28,29].

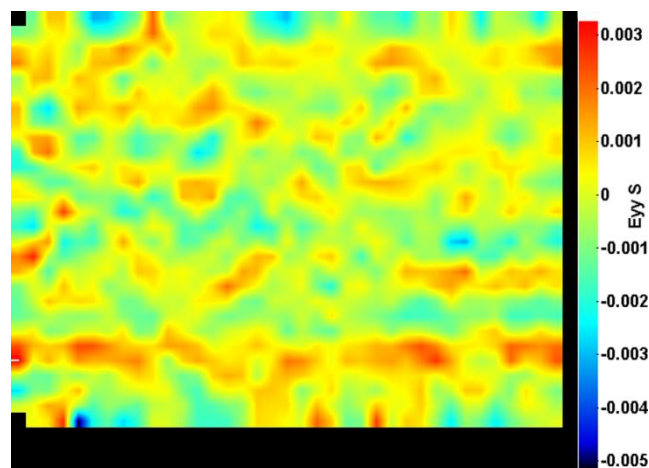


Fig. 8 The strain error due to the electron beam shift determined with DIC

The total error for strain values calculated using DIC have been estimated by computing the difference between the strain maps obtained for DIC (Fig. 5) and microgrids (Fig. 6) techniques. The error values obtained from Fig. 7 and 8 have also been included in the

calculations and results are shown in Fig. 9. Average strain values determined by both the DIC and microgrid techniques along the various rows of the deformed microgrids have also been calculated to compare the strain distribution pattern, Fig. 9-a. The error distribution curve in Fig. 9-a corresponds to the difference between the average strain values calculated with the two techniques and the broken line represents the total average error for the entire region. Fig. 9-a indicates that the strain distributions in the microstructure obtained from both techniques follow a very similar pattern. However, the DIC technique under-determines the strain values with an average error of about 16% for the amount of deformation applied during the test on IF steel. Similar error levels are also reported in the literature even for smaller applied strain [5,23] and infinitesimal strain values[18]. The error distribution map superimposed onto the deformed microstructure in Fig. 9-b shows that the largest errors are located where deformation is highly localized in the microstructure with shearing taking place, as highlighted by arrows in Fig. 3-b. Here the local error values as high as 34% are obtained when using DIC.

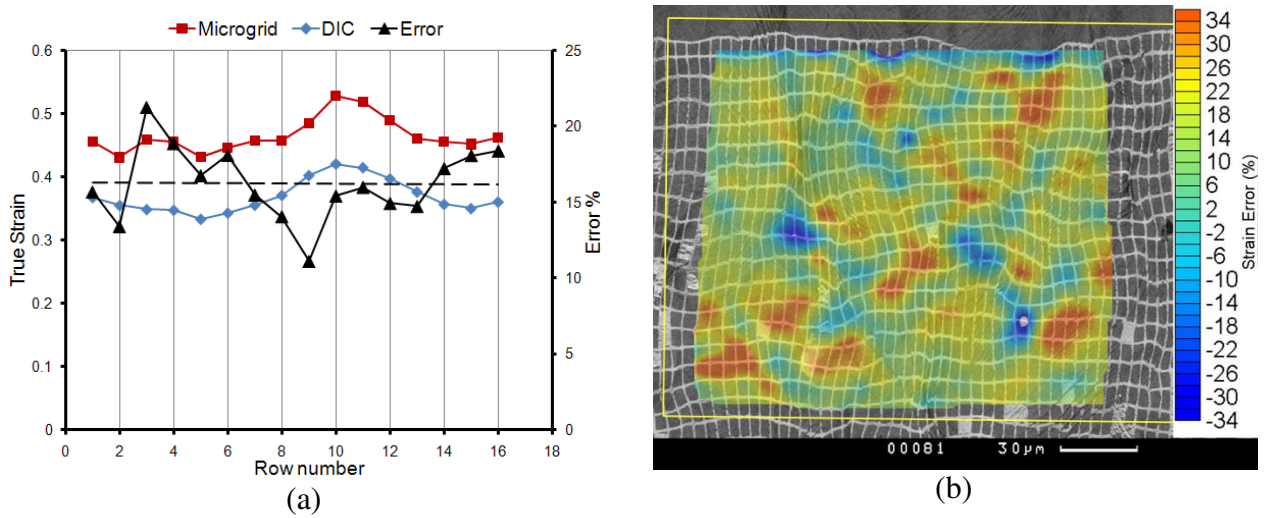


Fig. 9 (a) average strain values computed using DIC and microgrid techniques along the 16 rows of the microgrid together with the calculated errors and (b) error distribution for the entire analysed region

Although there is a wide range of error values, their distribution in magnitude for the entire analysed region, Fig. 10, shows that the values lie within the range of 0-34% for 80% of the total number of calculation points,. It is also found that the highest frequency occurs at the error value of about 17%, which correlates well with the average error values obtained from Fig. 9-a.

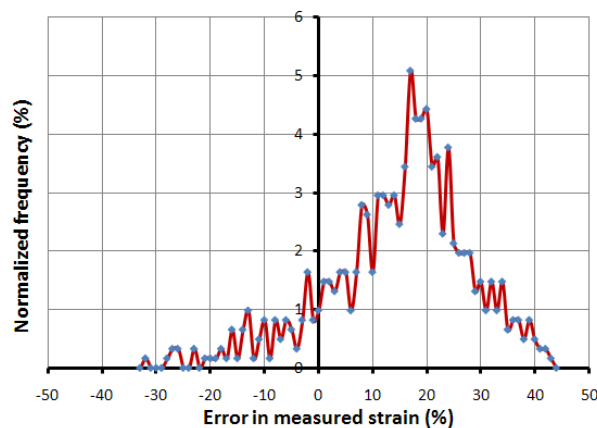


Fig.10 Distribution of errors across the entire analysed region of the microstructure

The error distribution pattern in Fig. 9-b indicates that the accuracy of the correlation process is reduced due to severe deformation localization associated with the emergence of local shear bands that affect the pattern tracked by the software as well as the local conditions of brightness and contrast. Despite the identified errors in the strain calculations from the DIC technique at the scale of microstructure, it is found that in the absence of severe local shearing, the technique can produce local strain measurements of a reasonable accuracy with mean error of about 16% for an applied tensile strain of 0.73 on IF steel.

The similarity of the strain distribution patterns between DIC and microgrid techniques shows that DIC measurements can reliably provide qualitative information about strain localization at the local scale and therefore, can help the understanding of microstructure evolution leading for instance to damage in the material. However, strain values, which depend on the selected correlation parameters, can be subjected to very large errors that can only be estimated using independent techniques.

5 Conclusions

Both DIC and microgrid techniques have been used to analyse the large local deformation of a single phase automotive steel at the scale of its microstructure during in-situ tensile testing. Local strain values of up to 0.9 and 0.7 have been measured using the microgrid and DIC techniques respectively for an applied global strain of 0.73. A procedure has been developed to quantify errors associated with the DIC strain measurements when the microstructural features of the material are used for the image correlation. Results have revealed that the strain distribution patterns obtained from DIC are in a reasonable agreement with those determined by using the microgrid technique. However, an average error of about 16% in strain values was found over the entire analysed area and a maximum error of about 34% was observed where the deformation is highly localized. The practical range of error values was found to be 0-34% for the analysed region. These results show that the DIC technique can be used to measure local strain values at the scale of microstructure with reasonable accuracy. However, independent techniques such as microgrids are needed to estimate errors for more quantitative measurements.

Acknowledgements

This research was carried out under project number M41.2.10398 in the framework of the Research Program of the Materials innovation institute M2i (www.m2i.nl). The authors would also like to thank EPSRC (grant number EP/F023464/1) for financial support and Tata Steel RD&T, IJmuiden in the Netherlands for providing the material of this study.

References

1. Asgari SA, Hodgson PD, Yang C, Rolfe BF (2009) Modelling of advanced high strength steels with the realistic microstructure-strength relationships. *Computational Materials Science* 45 (4):860-866
2. Ososkov Y, Wilkinson DS, Jain M, Simpson T (2007) In-situ measurement of local strain partitioning in a commercial dual phase steel. *International Journal of Materials Research* 98 (8):664-673
3. Jin H, Lu W-Y, Korellis J (2008) Micro-scale deformation measurement using the digital image correlation technique and scanning electron microscope image. *Journal of Strain Analysis for Engineering Design* 43 (8):719-728

4. Quinta Da Fonseca J, Mummery PM, Withers PJ (2005) Full-field strain mapping by optical correlation of micrographs acquired during deformation. *Journal of Microscopy* 218 (1):9-21
5. Kang J, Jain M, Wilkinson DS, Embury JD (2005) Microscopic strain mapping using scanning electron microscopy topography image correlation at large strain. *Journal of Strain Analysis* 4 (6):559- 570
6. Ghadbeigi H, Bradbury SR, Pinna C, Yates JR (2008) Determination of micro-scale plastic strain caused by orthogonal cutting. *International Journal of Machine Tools and Manufacture* 48 (2):228-235
7. Soppa E, Doumalin P, Binkele P, Wiesendanger T, Bornert M, Schmauder S (2001) Experimental and numerical characterisation of in-plane deformation in two-phase materials. *Computational Materials Science* 21 (3):261-275
8. Kang J, Ososkov Y, Embury JD, Wilkinson DS (2007) Digital image correlation studies for microscopic strain distribution and damage in dual phase steel. *Scripta Materialia* 56 (11):999-1002
9. Allais L, Bornert M, Bretheau T, Caldemaison D (1994) Experimental characterization of the local strain field in a heterogeneous elastoplastic material *Acta Metallurgica et Materialia* 42 (11):3865-3880
10. Obata M, Shimada H, Kawasaki A (1983) Fine- grid method for large strain analysis near a notch tip. *Experimental Mechanics* 23 (2):146-151
11. Koshelev PF, Sanderov V, Tsaref VN (1976) Investigation of deformation by a grid method. *Industrial Laboratory* 42 (6):963- 965
12. Karimi A (1984) Plastic flow study using the microgrid technique. *Materials Science and Engineering* 63 (22):267- 276
13. Delaire F, Raphanel JL, Rey C (2000) Plastic heterogeneities of a copper multicrystal deformed in uniaxial tension: experimental study and finite element simulations. *Acta Materialia* 48 (5):1075-1087
14. Sadat AB, Reddy MY (1989) Plastic strain analysis of the machined surface region using fine grid etched by photoresist technique. *Experimental Mechanics* 25 (3):346- 349
15. Sun S, Shiozawa K, GU J, Chen N (1995) Investigation of deformation field and hydrogen partition around crack tip in FCC single crystal. *Metallurgical and Materials Transaction A* 26 (3):731- 738
16. Ghadbeigi H (2010) Metal cutting mechanics: investigation and simulation of deformation and damage mechanisms. Ph.D. Thesis, The University of Sheffield, Sheffield
17. Sutton MA, Wolters WJ, Peters WH, Ranson WF, McNeill SR (1983) Determination of displacements using an improved digital image correlation method. *Image and Vision Computing* 1 (3):133-139
18. Chu TC, Ranson WF, Sutton MA, Peters WH (1985) Application of digital image correlation techniques to experimental mechanics. *Experimental Mechanics* 25 (2):232-244
19. Wattrisse B, Chrysochoos A, Muracciole JM, Nemoz-Gaillard M (2001) analysis of strain localization during tensile tests by digital image correlation. *Experimental Mechanics* 21 (1):29-39
20. Tarigopula V, Hopperstad OS, Langseth M, Clausen AH, Hild F, Lademo O-G, Eriksson M (2008) A study of large plastic deformation in dual phase steel using digital image correlation and FE analysis. *Experimental Mechanics* 48 (2):181-196
21. Pan B, Kemaq Q, Huimin X, Asundi A (2009) Two dimensional digital image correlation for in-plane displacement and strain measurement: a review. *Measurement Science and Technology* 20 (6):1-17
22. Sun Z, Lyons JS, McNeill SR (1997) Measuring microscopic deformations with digital Image correlation. *Optics and Laser in Engineering* 27 (4):409-428
23. Lagattu F, Bridier F, Villechaise R, Brillaud J (2006) In-plane strain measurements on a microscopic scale by coupling digital image correlation and an in situ SEM technique. *Materials Characterization* 56 (1):10-18
24. Tatschl A, Kolednik O (2003) A new tool for the experimental characterization of micro-plasticity. *Materials Science and Engineering A* 339:265- 280

25. Pan B, Asundi A, Huimin X, Gao J (2009) Digital image correlation using iterative least squares and pointwise least squares for displacement field and strain field measurement. *Optics and Laser in Engineering* 47 (7-8):865-874
26. Sutton MA, Mingqi C, Peters WH, Chao YJ, McNeill SR (1986) Application of an optimized digital correlation method to planar deformation analysis. *Image and Vision Computing* 4 (3):143-150
27. Jin H, Haldar S, Bruck HA, Lu W-Y (2011) Grid method for microscale discontinuous deformation measurement. *Experimental Mechanics* DOI:10.1007/s11340-01-9459-7
28. Sutton MA, Li N, Joy DC, Reynolds AP, Li X (2007) Scanning electron microscopy for quantitative small and large deformation measurements part I: SEM imaging at magnifications from 200 to 10,000. *Experimental Mechanics* 47 (6):775-787
29. Sutton MA, Li N, Garcia D, Cornille N, Orteu JJ, McNeill SR, Schreier HW, Li X, Reynolds AP (2007) Scanning Electron Microscopy for quantitative small and large deformation measurements part II: Experimental validation for magnifications from 200 to 10000. *Experimental Mechanics* 47 (6):789-804
30. Wang H, Xie H, Ju Y, Duan Q (2006) Error analysis of digital speckle correlation method under scanning electron microscope. *Experimental Techniques* 30 (2):42-45
31. Ghadbeigi H, Pinna C, Celotto S, Yates JR (2010) Local plastic strain evolution in a high strength dual phase steel. *Materials Science and Engineering A* 527 (18-19):5026-5032
32. Vander Voort GF (2000) *Metallography Principles and Practice*. ASM International, NewYork
33. LAVision (2005) *DaVis StrainMaster Software*.
34. Bornert M, Bremand F, Doumalin P, Dupre JC, Fazzini M, Grediac M, Hild F, Mistou S, Orteu JJ, Robert L, Surrel Y, Vacher P, Wattrisse B (2009) Assessment of digital image correlation measurement errors: methodology and results. *Experimental Mechanics* 49 (3):353-370